Spin fluctuations in random magnetic-nonmagnetic two-dimensional antiferromagnets. I. Dynamics

R. A. Cowley* and G. Shirane
Department of Physics, Brookhaven National Laboratory,† Upton, New York 11973

R. J. Birgeneau
Department of Physics, Massachusetts Institute of Technology,‡ Cambridge, Massachusetts 02139

H. J. Guggenheim
Bell Laboratories, Murray Hill, New Jersey 07974

(Received 26 October 1976)

The magnetic excitations in the system $Rb_2Mn_cMg_{1-c}F_4$ with $c = 1$, 0.57, and 0.54 have been measured using neutron-inelastic-scattering techniques. In pure Rb_2MnF_4 the magnon dispersion relation is accurately described by simple spin-wave theory with dominant Heisenberg antiferromagnetic nearest-neighbor exchange, a much weaker antiferromagnetic next-nearest-neighbor interaction, and a small single-ion anisotropy field. In the specimens with $c = 0.57$ and 0.54 the scattering shows a broad response but with substructure which may be associated with the different Ising energies of Mn ions in different environments. The measurements are in excellent accord with the results of computer simulations but theories based on the coherent-potential approximation do not give a satisfactory description of the measured spectra.

I. INTRODUCTION

In the past several years a number of studies of the dynamics of concentrated insulating magnetic alloys have been reported.[1] The explicit systems studied have been almost exclusively transition-metal-fluoride binary alloys with the transition-metal constituents either both magnetic or magnetic-nonmagnetic. The reasons for this ubiquitous choice of these fluoride hosts are (i) the transition-metal ions are all quite similar chemically so that true random alloys can be synthesized with little or no clustering effects, while at the same time, the ions may be quite dissimilar magnetically. (ii) The exchange interaction is typically isotropic and between nearest neighbors only; thus, the mixed-crystal Hamiltonian involves only a small number of parameters all of which are known from measurements on the pure systems and/or very dilute alloys. (iii) The spin-wave energies are in the range most easily measured by conventional neutron-scattering techniques. (iv) In favorable cases large homogeneous single crystals may be grown, so that the dynamic structure factor[2] $S(\vec{Q}, \omega)$ may be measured with high resolution throughout the Brillouin zone. All of these factors combine to produce a nearly ideal situation in which a direct confrontation between experiment and theory is possible.

The current status of experiment and theory in these substitutionally disordered fluorides has been summarized by Cowley.[1] For the mixed magnetic systems, experiments on real crystals, computer-simulation experiments,[3,4] and various analytic theories, most notably those based on the coherent-potential approximation[5,6] (CPA), seem to be in general accord. The most glaring discrepancy is in the intensities at low frequencies and small wave vectors in the two-dimensional (2-D) mixed antiferromagnet $Rb_2Mn_{0.5}Ni_{0.5}F_4$.[7] In that case there is much more weight at long wavelengths than predicted by any of the theories including the computer simulations. Als-Nielsen *et al.*[7] have also shown that in $Rb_2Mn_{0.5}Ni_{0.5}F_4$, the static critical behavior is identical to that in the pure systems.

The situation in mixed magnetic-nonmagnetic systems is rather more complex. Whereas in mixed magnetic systems the excitations split into two well-defined branches, in the dilute Heisenberg magnets $S(\vec{Q}, \omega)$ generally becomes much broader and ill-defined[8]; thus it is less meaningful to talk in terms of spin waves or a "dispersion relation." Correspondingly, the CPA theories are more difficult for dilute systems as compared to mixed magnetic systems. Until recently, one of the principal issues in these random crystal studies was the existence or nonexistence of residual structure in the overall broad response; this substructure represents the remnants of the Ising cluster modes reflecting the different possible environments of the magnetic ion. Very recent high-resolution experiments on $Mn_cZn_{1-c}F_2$,[9] however, indicate that there is indeed some barely resolvable structure in $S(\vec{Q}, \omega)$, in that system at least, at wave vectors near the magnetic zone boundary.

The most subtle, and certainly the least understood aspects of dilute magnets, relate to percolation[10,11] rather than to the dynamics. It has already been shown in a number of experiments in the transition-metal fluorides[12] that when the magnetic ion concentration c is reduced below a certain level, the system does not order down to very low temperatures, that is, there is no long-range order down to at least 1 K. This almost certainly corresponds to the classical percolation problem. In this case for nearest-neighbor interactions alone and for $c < c_p$, the percolation concentration, the system breaks up into finite clusters. As $T \to 0$, these clusters will freeze into some static configuration, but the different clusters will be statistically uncorrelated. There is currently virtually no experimental information on the temperature dependence of the correlations in real magnets near the percolation concentration. Similarly, rather little is known about the long-wavelength dynamics in these percolative clusters.

Motivated by the above considerations, we have undertaken an extensive study of the mixed magnetic-nonmagnetic 2-D antiferromagnets $Rb_2Mn_cMg_{1-c}F_4$. These are isomorphous to the much studied pure antiferromagnets K_2NiF_4, Rb_2MnF_4, etc. Previously, detailed experiments have been performed on the mixed magnetic system $Rb_2Mn_{0.5}Ni_{0.5}F_4$,[7] and this present work represents an extension of that to the diluted case, as well as an extension to two dimensions of earlier studies on the three-dimensional (3-D) magnets $Mn_cZn_{1-c}F_2$.[1,8,9]

Our experiments subdivide straightforwardly into two distinct categories: (i) those concerned with the general dynamical response $S(\vec{Q}, \omega)$ across the Brillouin zone at low temperatures, and (ii) studies of the static temperature and concentration-dependent correlations for samples with $c \sim c_p$ together with some high-resolution measurements of the long-wavelength dynamics. The main advantage of the system, $Rb_2Mn_cMg_{1-c}F_4$, for part (i) is that for the simple square lattice $Z = 4$ the near-neighbor coordination is quite low. This, in turn, implies that the "Ising cluster modes" which are a very subtle feature in the $Mn_cZn_{1-c}F_2$ system should become a gross feature of the dynamics here.[3,4,6,8] As we have indicated above, there is almost no experimental information in the literature on the correlations near percolation. The main advantage of these 2-D systems is that in two dimensions the deviation from mean-field behavior is as large as it can be in the percolation problem.[13] Thus, these experiments should provide important information to guide and select between theories of magnetism around the percolation point. We have, in fact, already published a brief note on certain aspects of the percolation work.[14]

In this paper we discuss our experiments and theory for the dynamics in $Rb_2Mn_cMn_{1-c}F_4$. In a second paper to follow this, (hereafter labeled II) we give a complete description of the percolation experiments. The format of this paper is as follows. In Sec. II we describe the sample characterization, crystal and magnetic structure, and other basic details. Section III describes measurements of the spin-wave dispersion relations in the pure material Rb_2MnF_4. These are a necessary prerequisite to our detailed studies of the dilute samples. The measurements on the dynamics of the dilute crystals are given in Sec. IV. A detailed comparison with computer simulation and CPA theories is made in Sec. V. Finally, the conclusions are given in Sec. VI.

II. PRELIMINARY DETAILS

A. Crystal growth

In order to grow large single crystals that are random and whose final composition corresponds closely to that desired, considerable care must be taken in the growth technique. The need for especially large crystals in these dynamic studies has therefore led us to explore new methods of crystal growth for this family of compounds. We have indeed developed a new technique which has been quite successful. We describe this very briefly below. A full report will be given elsewhere.[15]

In the past, crystals of Rb_2XF_4 (X = Ni or Mn) were prepared primarily by horizontal zone melting or the Bridgman method.[15] Because these compounds melt incongruently, the general method of preparation has been the mechanical separation of the 2-D phase from the other phases after growth. While this technique often produced good material, the single crystal size was almost always rather less than 1 cm^3 in volume. As noted above, rather larger crystals are required for studies of the sort reported in this paper. Recently, we have found that by using a mixture containing an excess of RbF (40 mole%), the phase equilibria are shifted sufficiently to produce Rb_2XF_4 as the first phase to solidify. Therefore, good single crystals could be grown on an oriented seed crystal. This was done by using the Czochralski pull method. A typical crystal preparation was as follows. A mixture of single crystals of RbF, MnF_2, and MgF_2 (each previously zone refined) was weighted to produce the stoichiometric equivalent of $Rb_2Mn_cMg_{1-c}F_4$ plus 40 mole% excess RbF. This mixture was melted in a platin-

um boat in a hydrogen fluoride atmosphere. The charge was then transferred to a vitreous carbon crucible in a crystal puller. A quartz envelope was used to contain a nitrogen atmosphere. A crystal was pulled on a seed crystal at 1-5 mm/h with a rotation speed of 20–50 revolutions per minute.

B. Sample characterization

For these studies we grew crystals with three nominal compositions: Rb_2MnF_4, $Rb_2Mn_{0.59}Mg_{0.41}F_4$, and $Rb_2Mn_{0.50}Mg_{0.50}F_4$. Several boules of each were grown and individual samples with optimal mosaic spread and size were selected for detailed study. The crystals were typically 2 cm^3 in volume and had a mosaic spread of several minutes. In general, the crystals have a laminar morphology. Typical Bridgman crystals (for example, the $Rb_2Mn_{0.5}Ni_{0.5}F_4$ described in Ref. 7) actually consist of a large number of slightly misaligned platelets. This platelet stratification was much less pronounced in these pulled crystals.

We now consider our estimates of the actual versus the nominal concentration, in two samples, one nominally 50% Mn and the second nominally 59%. From previous studies of random fluorides one knows that the final composition may differ markedly from the composition of the starting material. Further, from the work on $Rb_2Mn_{0.5}Ni_{0.5}F_4$ and $Mn_cZn_{1-c}F$, we know that the composition may vary across the boule itself by as much as 10%. Chemical analysis of separate samples taken from the 50% and 59% boules yielded actual Mn atomic concentrations of 55% and 60.5%, respectively. As discussed in Ref. 14, we know that the 60.5% estimate must be slightly high for the "59%" neutron sample since the neutron studies of the spin fluctuations in the nominal 59% sample show that there is no magnetic long-range order down to 1 K. This in turn necessitates that $c < c_p = 0.59$. The simplest method of estimating the concentration is from the lattice constant themselves. We show in Table I the measured lattice constants at 5 K for our samples. All three samples were confirmed to have the K_2NiF_4 structure.[16] At room temperature $a(Rb_2MnF_4) - a(Rb_2MgF_4) = 0.17$ Å so that the mixed samples have lattice constants in the range expected on the basis of the nominal concentrations. From Table I we can estimate accurately that the two mixed samples differ by 3% in Mn concentration (as opposed to 9% nominally, and (5 ± 2)% from the chemical analysis on the separate samples). We should add that this interpolation technique is not reliable enough to give accurate absolute concentrations.

TABLE I. Lattice constants at 5 K.

	a (Å)	c (Å)
Rb_2MnF_4	4.2153(8)	...
$Rb_2Mn_{0.57}Mg_{0.43}F_4$	4.1500(4)	13.801(15)
$Rb_2Mn_{0.54}Mg_{0.46}F_4$	4.1457(4)	13.801(15)

After some study we realized that the concentrations of the explicit samples studies could be estimated most accurately from our own quasielastic neutron-scattering measurements. In particular the pair-connectivity correlation length as measured in Ref. 14 depends sensitively on the Mn^{++} concentration. As discussed extensively in Paper II and briefly in Ref. 14, this technique yields $c = 0.54 \pm 0.01$ and $c = 0.57 \pm 0.01$ for the two samples. The former value, $c = 0.54$, is satisfactorily close to the chemical analysis result of $c = 0.55 \pm 0.02$ while the difference value of 3% agrees exactly with out lattice-constant estimate. Also, as discussed in Sec. V of this paper, if one regards c as an adjustable parameter in fitting computer simulation theory to the measured zone boundary $S(\vec{Q}, \omega)$, then one obtains independent estimates of $c = 0.54 \pm 0.03$ and $c = 0.57 \pm 0.03$ in the two samples. Clearly, neither of these estimates is theory independent, but the close internal agreement, together with the reasonable consistency with the chemical analysis, leads us to believe that they are quite accurate. Henceforth, we refer to the separate samples studied as "*concentrated, 57% and 54%.*"

C. Crystal and magnetic structure; randomness

The crystal and magnetic structures of Rb_2MnF_4, together with the (010) and (001) magnetic zones of the reciprocal lattice, are shown in Fig. 1. In all cases only those nuclear Bragg peaks appropriate to the K_2NiF_4 structure are observed, thereby confirming that the mixed crystals do indeed retain the pure crystal structure. The magnetic ordering in Rb_2MnF_4 has been extensively discussed by Birgeneau *et al.*[17]; the spin waves and sublattice magnetization have been discussed by de Wijn *et al.*[18] Above $T_N = 38.4$ K, Rb_2MnF_4 exhibits pronounced 2-D magnetic short-range-order effects in which near neighbors are antiferromagnetically aligned. This short-range order manifests itself as lines of diffuse magnetic scattering in the (010) zone extending in the l direction along $[h0l]$, centered about $h = 1, 3, \ldots$. At $T_N = 38.4$ K the system undergoes a rather unusual phase transition to 3-D magnetic order. In the same crystal, Birgeneau *et al.*[17] observe two distinct 3-D ordering patterns. In the first, which is illustrated in Fig. 1, the central spin on the

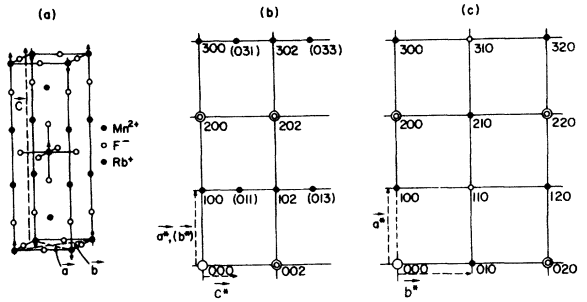

FIG. 1. (a) Crystal and magnetic structures of Rb_2MnF_4. Inverting the central spin exchanges the $\vec{a}$ and $\vec{b}$ magnetic axes. Here we show only the K_2NiF_4-type magnetic structure; the Ca_2MnO_4-type structure may be generated by inverting the spins of the nnn layer. (b) (010) and (100) magnetic zones of the reciprocal lattice; again we show only K_2NiF_4-type Bragg positions. Nuclear Bragg peaks are indicated by double circles. (c) (001) zone of the reciprocal lattice: K_2NiF_4-type magnetic scattering is observed only at the filled-circle positions.

near-neighbor (nn) plane may point either up or down, while the spins along the c axis of next-nearest-neighbor (nnn) planes are parallel. This gives rise to the magnetic superlattice peaks shown in Figs. 1(b) and 1(c). This magnetic structure is commonly denoted as the K_2NiF_4 structure. However, a second structure also occurs in which the spins of nnn planes along the c axis are antiparallel (the so-called Ca_2MnO_4 structure[19]). This gives rise to superlattice scattering at $(h, k, \frac{1}{2}l)$ with $h+k, l$ odd. These two structures otherwise have identical magnetic properties, thereby showing that the magnetism is determined completely by the 2-D in-plane interactions. In the diluted crystals since $c < c_p = 0.59$ no magnetic Bragg scattering is anticipated. However, there should be lines of diffuse magnetic scattering along $[h0l]$, reflecting the development of magnetic correlations in the percolation clusters, in exact correspondence to the critical scattering in the concentrated system. This diffuse scattering is the subject of Paper II.[14]

Finally, we must consider the degree of randomness in the mixed crystals. As we noted in the introduction, Mn^{++} and Mg^{++} are quite similar chemically so no pronounced clustering is anticipated. A variety of neutron scans were made in exact analogy with those described by Als-Nielsen *et al.*[7] in their crystallographic characterization of $Rb_2Mn_{0.5}Ni_{0.5}F_4$. As in that case, and in the case of $Mn_cZn_{1-c}F_2$,[8] we find a null result; that is, we see no features in the diffuse background scattering indicative of positional short-range-order effects. We conclude therefore that the Mn^{++} and Mg^{++} are indeed randomly distributed.

III. MAGNETIC INTERACTIONS IN Rb_2MnF_4

Since the interpretation of our measurements on the system $Rb_2Mn_cMg_{1-c}F_4$ requires a knowledge of the exchange interactions between the Mn^{++} ions, we have measured the spin-wave excitations in a crystal of pure Rb_2MnF_4. The experiments were performed at the Brookhaven high flux Beam Reactor. The crystal at 4.5 K was oriented with a c axis vertical on a triple-axis crystal spectrometer; measurements were thus in the (001) zone [Fig. 1(c)]. The measurements were performed with pyrolytic graphite crystals as both monochromator and analyzer and a constant incident neutron energy of 14.8 meV. A pyrolytic graphite filter was used to reduce the higher-energy contaminants in the incident neutron beam. The collimation was typically 10 min throughout.

As discussed in Sec. II, the magnetic ordering in Rb_2MnF_4 has been described by Birgeneau *et al.*[17] Above 38.4 K there are 2-D magnetic short-range ordering effects in which the near neighbors are antiferromagnetically aligned. At 38.4 K the system undergoes a transition to a 3-D magnetically ordered structure which may take one of two forms, dependent upon the relative orientation of the magnetic planes along the c axis. In our specimen, magnetic Bragg reflections were observed at 100 and 010 reciprocal-lattice points showing that at least part of the crystal ordered with the K_2NiF_4 structure which is illustrated in Fig. 1.

The frequencies of the spin waves were determined for propagation directions $[\zeta 00]$, $[\zeta\zeta 0]$, and $[\zeta\, 0.5\, 0]$ $(\zeta = aq/2\pi)$ within the magnetic unit cell shown in Fig. 1. Some typical scans are shown in Fig. 2 where the widths of the groups are consistent with the expected instrumental

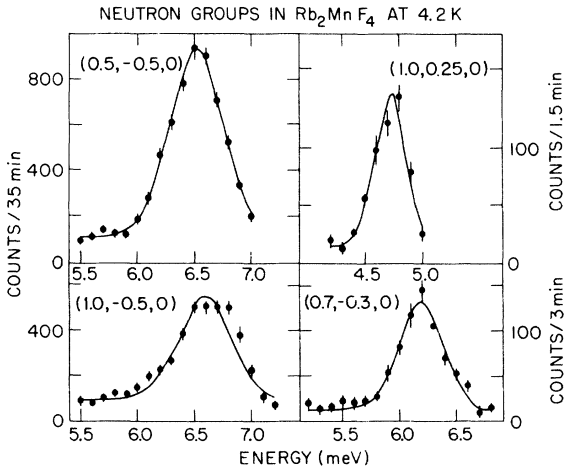

FIG. 2. Typical neutron groups for spin waves at 4.2 K in Rb_2MnF_4. The widths are determined by the resolution of the spectrometer.

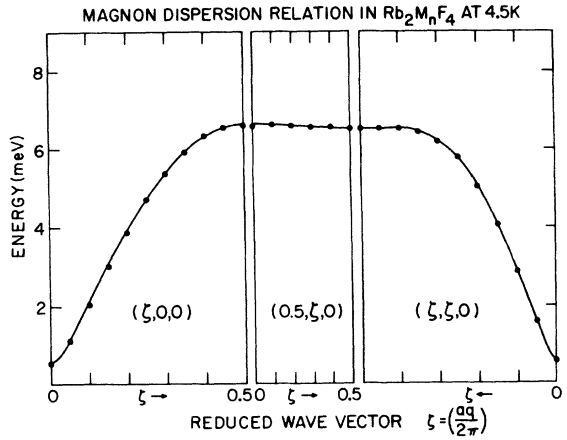

FIG. 3. Magnon dispersion relation at 4.2 K in Rb_2MnF_4. The solid line is the best-fit theoretical dispersion wave using the parameters listed in Table II including J_1 and J_2 and (model II).

resolution. The frequencies of the spin waves were determined by fitting, in a least-squares sense, Gaussians to the neutron groups, and the resulting frequencies are shown in Fig. 3. In all cases the relative errors are smaller than the size of the points on the dispersion curve. At the magnetic zone center the measured energy, 0.62 ± 0.02 meV, is in excellent accord with the result obtained by antiferromagnetic resonance techniques,[20] 0.62 ± 0.005 meV.

Spin-wave theory for Rb_2MnF_4 has been extensively discussed by de Wijn *et al.*[18] These authors have deduced the nearest-neighbor-exchange constant from measurements of the sublattice magnetization. We have assumed a model which includes nearest-neighbor exchange J_1 and next-nearest-neighbor exchange J_2 within the magnetic planes; the anisotropy originating from the magnetic dipolar interactions is incorporated as an anisotropy field. The Hamiltonian is then given by

$$\mathcal{H}=J_1\sum_{\langle nn\rangle}\vec{S}_i\cdot\vec{S}_j+J_2\sum_{\langle nnn\rangle}\vec{S}_i\cdot\vec{S}_j - g\mu_B H_A\sum_i(-1)^i S_i^x\,, \qquad (1)$$

where all the sites on one magnetic sublattice have i even and the others have i odd, and the summations are over nearest-neighbor and next-nearest-neighbor pairs.

The energies of the spin waves of wave vector $\vec{q}$ are then obtained from linear spin-wave theory as

$$E_{\vec{q}}/4SJ_1=\{[1+\alpha+\beta\gamma_2(\vec{q})]^2-\gamma_1(\vec{q})^2\}^{1/2}\,, \qquad (2)$$

where

$$\alpha=g\mu_B H_A/4J_1S,\quad \beta=J_2/2J_1\,,$$

and

$$\gamma_1(\vec{q})=\cos(\tfrac{1}{2}q_x a)\cos(\tfrac{1}{2}q_y a)\,,$$

$$\gamma_2(\vec{q})=\cos(q_x a)+\cos(q_y a)-2\,.$$

A least-squares fit to the experimental results shown in Fig. 3 was performed neglecting the next-neighbor-exchange interactions. The results are shown in Table II where they are compared with the values deduced by de Wijn *et al.*[18] The results are in remarkably good agreement with one another.

More distant interactions might play an important role in determining the behavior of the magnetic correlations near the percolation point; as noted previously, the critical percolation concentration on a square lattice is 0.59 for nearest-neighbor interactions,[10] and 0.41 for next-nearest-neighbor interactions. Consequently, one of the principal objectives of our study of Rb_2MnF_4 was to determine the magnitude of the $\langle nnn\rangle$ exchange interactions. This is most readily observed by comparing the energies of the spin waves for wave vectors at the $[\zeta 00]$ and $[\zeta\zeta 0]$ zone boundaries. The difference between these two frequencies is given within the linear spin-wave approximation as

$$E(\tfrac{1}{2},0,0)-E(\tfrac{1}{2},\tfrac{1}{2},0)=2J_2S\,.$$

Both of these frequencies were determined at a variety of different wave-vector transfers, two of which are illustrated in Fig. 2. The resulting estimate for β from the difference between the

TABLE II. Parameters of the spin-wave dispersion relation in Rb_2MnF_4.

Parameters	Model I	Model II	de Wijn *et al.*[18]
J_1 (meV)	0.6544 ± 0.0014	0.6734 ± 0.0028	0.657 ± 0.008
α	0.0048 ± 0.0010	0.0048 ± 0.0007	0.0047
β	0	0.0088 ± 0.0013	0
Goodness of fit χ^2	0.016	0.005	

values is $\beta = 0.010 \pm 0.003$. An alternative estimate of β was obtained by a least-squares fit to all the measurements shown in Fig. 3. The results are listed in Table II and give $\beta = 0.0088 \pm 0.0013$.

One possible origin of the next-nearest-neighbor interaction in Rb_2MnF_4 is the magnetic dipolar forces. These interactions are discussed in detail by de Wijn *et al.*[18] who calculate the lattice sums for this structure. Their calculations show that the dipolar forces split the degeneracy of the zone-boundary modes at the $[\zeta\zeta 0]$ zone boundary; the splitting is 0.08 meV and the mean energy is reduced by 0.006 meV. The energy of the excitations at the $[\zeta 00]$ zone boundary is reduced by 0.009 meV. We conclude that dipolar forces give rise to a difference between the energies of the two zone boundaries which is the opposite sign and an order of magnitude smaller than we observe. Consequently, the measurements show there to be a next-nearest-neighbor antiferromagnetic exchange interaction $J_2 = 0.012 \pm 0.002$ meV. The nearest-neighbor-exchange interaction is 0.673 ± 0.028 meV which when corrected for the effects of spin-wave interactions[18] gives an exchange constant of 0.653 ± 0.027 meV.

IV. DYNAMICS OF EXCITATIONS IN $Rb_2Mn_cMg_{1-c}F_4$

The experiments were carried out with the same experimental configuration as described above except that coarser collimation was employed. The collimation before the monochromator was 20 min, and after the monochromator, and both before and after the analyzer, was 40 min. The analyzer angle was held constant throughout the scans so that the outgoing neutron energy was 14.8 meV and a pyrolytic-graphite filter was inserted between the specimen and the analyzer to remove those neutrons which would be reflected by the higher-order reflections in the analyzer. In this configuration, the energy resolution of the spectrometer was typically 0.6 meV full width at half-maximum.

Spin-wave excitations may be measured using neutron scattering by means of the transverse part of the scattering cross section. If $\hbar\omega$ is the neutron energy loss and $\vec{Q}$ the neutron wave-vector transfer, the transverse part of the cross section for unpolarized neutrons is given by[2]

$$\frac{d^2\sigma^t}{d\Omega\, d\omega} = \left(\frac{\gamma e^2 g}{m_e c^2}\right)^2 \frac{k^1}{k_0} f^2(\vec{Q}) \tfrac{1}{4}\left(1 + \frac{Q_z^2}{\vec{Q}^2}\right) S^t(\vec{Q}, \omega)\,, \tag{3}$$

where $f(\vec{Q})$ is the form factor of the magnetic ions, and k_0 and k' are the wave vectors of the incident and scattered neutrons, respectively, and the spin direction has been taken to be the z axis. The Van Hove scattering function is given by

$$S^t(\vec{Q}, \omega) = \frac{1}{2\pi} \int_{-\infty}^{\infty} dt\; e^{i\omega t} \times \sum e^{i\vec{Q}\cdot(\vec{R}_m - \vec{R}_n)} \langle S_m^+(0) S_n^-(t) + S_m^-(0) S_n^+(t)\rangle\,, \tag{4}$$

where the summation is over all the magnetic sites at $\vec{R}_m$ or $\vec{R}_n$, and the spin variables have been written in the Heisenberg representation.

The crystals were oriented with [010] axis vertical [Fig. 1(b)] in a variable-temperature cryostat, and the spectrometer controlled in the constant-Q mode of operation with variable incident energy. Ideally, the intensity observed in each scan is then proportional to $S^t(\vec{Q}, \omega)$; the $1/k_0$ factor being cancelled by the $1/k_0$ efficiency of the monitor counter. In practice, however, the monochromator reflects neutrons with wave vectors proportional to $2k_0$, $3k_0$ and $4k_0$, as well as the desired neutrons with wave vector k_0. These contaminant neutrons are also counted, with steadily decreasing efficiency, by the monitor detector, and it is necessary to correct the observed spectra for the effect of these neutrons on the monitor. This correction was estimated as follows[21]: (i) by determining the number of higher-order neutrons using the absorption of different thicknesses of boron-loaded glass, (ii) by measuring the intensity of phonons in copper and comparing with the theoretical cross-section, and (iii) by measuring the magnons in K_2MnF_4,[22] and comparing the intensities with those expected for antiferromagnetic spin waves. The results of all these methods were in accord with one another to an accuracy of 5% for incident neutron energies between 10 and 40 meV. The correction factor relevant for this experiment is shown in Fig. 4 arbitrarily normalized to unity for an energy transfer of 6 meV.

Also shown in Fig. 4 are the observed distributions for the zone-boundary wave vector of $Rb_2Mn_{0.54}Mg_{0.46}F_4$ at three different temperatures, 1.1, 5.0, and 10.0 K. The background under the observed distributions is shown by the dotted lines and is believed to arise largely from the room background and to be independent of energy transfer. These results show that there is considerable magnetic scattering, but that it is spread between 0 and 7.5 meV. Within this frequency interval, however, the intensity is not constant but shows peaks at 3.15 ± 0.15, 4.85 ± 0.15, and 6.40 ± 0.15 meV. The frequencies of these peaks may be compared with the Ising frequencies rSJ of the Mn ions with the number of magnetic neighbors $r = 1, 2, 3$, and 4; namely, using the results of Table I: 1.63, 3.27, 4.90, and 6.55 meV. The

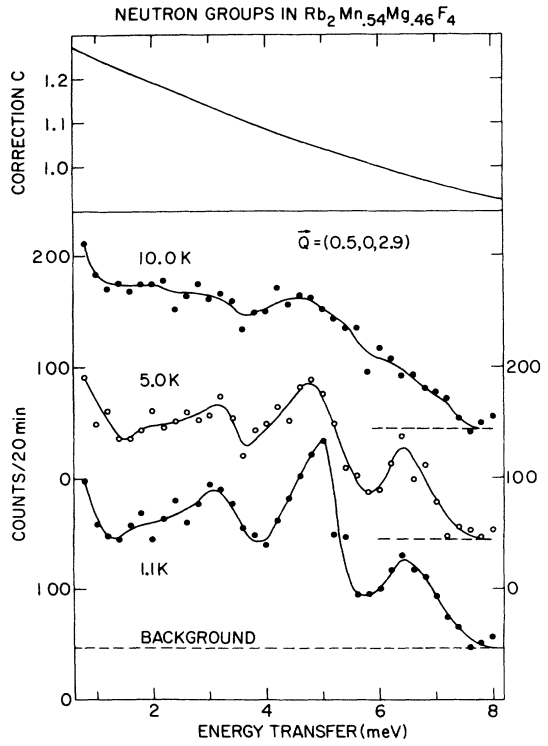

FIG. 4. Zone-boundary $S^t(\vec{Q}, w)$ in $Rb_2Mn_{0.54}Mg_{0.46}F_4$ as a function of temperature. The upper part of the figure gives the $\lambda/2$ correction factor C as discussed in the text. The solid lines are guides to the eye.

agreement between the positions of the peaks and these Ising frequencies suggests that the structure arises as a result of the characteristic frequencies of Mn ions surrounded by different numbers of neighbors. These results are qualitatively similar to those observed previously[9] in $Mn_{0.32}Zn_{0.68}F_2$ and $Mn_{0.68}Zn_{0.32}F_2$, but in the present case the structure is very much more pronounced and easier to measure experimentally. A large part of this is due to the fact that there are only five different possible configurations around each magnetic ion in this case, whereas there are nine in the rutile structure. Figure 4 also shows that there is a considerable temperature dependence to the structure. The peaks are less pronounced at 5.9 than at 1.1 K, and have almost disappeared at 10 K. This temperature dependence is correlated with the temperature dependence of the correlation length described in Paper II.

Measurements were made at six different wave vectors along the [ξ00] direction in the magnetic Brillouin zone in $Rb_2Mn_{0.54}Mg_{0.46}F_4$ crystal. Background was subtracted from the results and the correction applied for the effect of higher-order neutrons on the monitor. The results are shown in Fig. 5. As the wave vector decreases towards the zone center, the intensity of the scattering increases, and its weight moves to smaller energies. Both of these results are to be expected from a broadened antiferromagnetic spin-wave excitation. The fine structure, which is observed most clearly at the zone boundary, persists at all wave vectors, but is very much less pronounced at the zone center.

The energies at which the peaks and shoulders occur are shown in Fig. 6. There is little dispersion to the energies of the structure at the highest energies, but there is considerably more dispersion to the other bands. In Fig. 6, these frequencies are compared with the Ising energies calculated with the exchange constant appropriate for $Rb_2Mn_{0.54}Mg_{0.46}F_4$ as discussed in Sec. V A. The observed bands lie between the Ising energies and tend to lie just above an Ising energy at the zone center and just below the energy at the zone boundary.

Less-detailed measurements were made on the other sample $Rb_2Mn_{0.57}Mg_{0.43}F_4$, because the concentrations of the two samples are very similar, and no marked qualitative change in the spin-wave scattering with concentration was anticipated. The results for the zone-boundary response, after subtraction of the background and multiplication by the correction factor (Fig. 4), are shown in Fig. 7. Comparing this result with Fig. 5, indeed shows that there is little qualitative change in the scattering with concentration. As expected, in the more concentrated sample the weight of the scattering is moved somewhat to larger energies, but the energies of the peaks

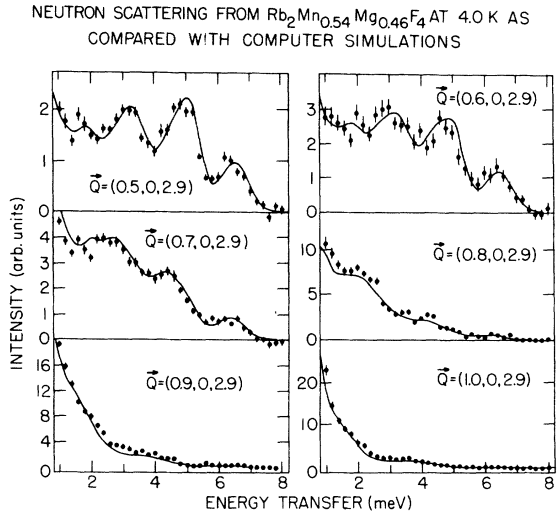

FIG. 5. Dynamical response $S^t(\vec{Q}, w)$ as a function of wave vector in $Rb_2Mn_{0.54}Mg_{0.46}F_4$. The solid lines are the Alben-Thorpe computer calculations as discussed in the text.

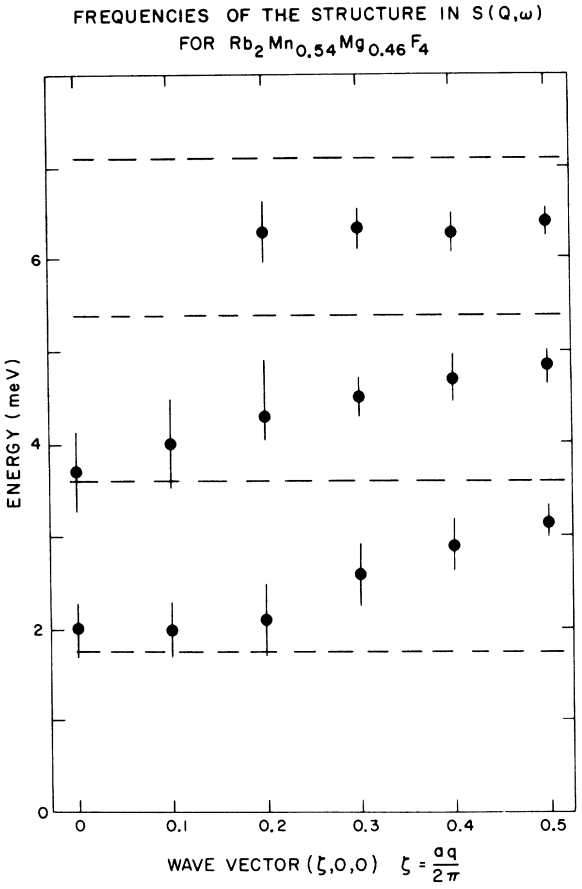

FIG. 6. Energies of the Ising peaks in $Rb_2Mn_{0.54}Mg_{0.46}F_4$ as a function of wave vector at 4.0 K.

3.05 ± 0.20, 4.95 ± 0.15, and 6.50 ± 0.15 are the same as those found in the $c = 0.54$ sample.

V. COMPARISON WITH THEORY

A. Computer simulations

The first computer simulations of disordered antiferromagnets were performed by Harris and Holcomb[4] for the $Mn_cZn_{1-c}F_2$ system. Since then such techniques have been used to study the $K_2Mn_cNi_{1-c}F_4$ system, and more recently the $Rb_2Mn_cMg_{1-c}F_4$ system.[3,4] Kirkpatrick and coworkers[4] calculate an expression for the neutron scattering by direct inversion of a large matrix. The procedure adopted by Thorpe and Alben[3] is more allied to molecular dynamics and involves integration of an equation of motion. Thorpe and Alben have kindly made their computer program available to us, and for this reason, we give a detailed comparison with results obtained using their techniques. From Ref. 4 we judge that closely similar, if not identical results, would be obtained using the Kirkpatrick method.

The computer simulation is begun by setting up an antiferromagnet arrangement of spins on a square lattice. Some of these spins are then removed using a random-number generator so as to give the desired concentration of magnetic and nonmagnetic sites. The excitations are then calculated by setting up a spin wave in the structure and numerically integrating the equation of motion of the spin wave which is deduced by using the normal approximations of linear spin-wave theory. The resulting time evolution is Fourier transformed to obtain the correlation function Eq. (4). As noted above, the calculation was performed with the aid of computer program supplied by Alben. The details are the same as these described by Thorpe and Alben[3] except that the damping function used in the Fourier transforms was $\exp(-\lambda t^2)$ instead of $\exp(-\lambda t)$. The former choice gives a Gaussian peak after Fourier transformation which more accurately simulates the experimental resolution function than the Lorentzian form used earlier. The parameter λ was chosen so that the width of the Gaussian was the energy resolution of the experiment.

The calculations were performed with a square lattice containing 80×80 sites and the time development followed for 91 time steps. The weak next-nearest-neighbor interaction (Sec. III) was neglected in the calculations, and the anisotropy field was chosen to have the same value as in Rb_2MnF_4. Initially the calculations were performed with the nearest-neighbor-exchange constant having the same value as in Rb_2MnF_4. The peaks in the structure were then all at significantly lower energies than those observed. In the final calculations the nearest-neighbor-exchange interaction was taken to be 0.72 meV and the results of the calculations are shown in Figs. 5 and 7. The overall intensity normalization of the theory to the experimental curves was determined by making the areas under the curves between 1.0 and 7.0 meV equal at a single q vector, in this case, the zone boundary. The calculated spectra at the other wave vectors shown in Fig. 5 were multiplied by the change in both the form factor and the geometric factor $(1 + Q_z^2/\vec{Q}^2)$ with wave-vector transfer. The inclusion of the geometric factor is appropriate, as will be shown in Paper II because the majority of the spins are aligned along the c [001] axis at low temperature. That is, the clusters simulate finite-size Néel antiferromagnets at the lowest temperatures; hence the inelastic scattering should be overwhelmingly transverse in character.

The agreement between the observations and the calculations shown in Figs. 5 and 7 is unusually gratifying. The calculations accurately reproduce

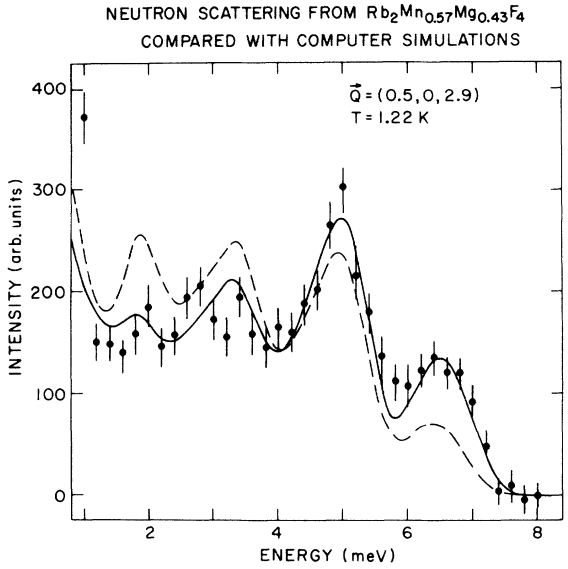

FIG. 7. Zone boundary $S^t(\vec{Q}, w)$ in $Rb_2Mn_{0.57}Mg_{0.43}F_4$ at 1.22 K. The solid and dashed lines are the Alben-Thorpe computer calculations for $c = 0.57$ and 0.50 respectively.

both the frequency dependence and intensity of the neutron scattering for all the measured wave vectors. This success shows that linear spin-wave theory is as appropriate for describing disordered systems as for pure systems.

In the calculations reported by Thorpe and Alben[3] for $c = 0.5$ and reproduced by the dotted line in Fig. 7, there is a sharp peak with an energy of approximately 1.7 meV, which they associate at least in part with the existence of isolated triads of magnetic ions. It is of interest that this peak is largely suppressed in both the experiment and the calculations when the concentration is increased to $c = 0.54$ or 0.57.

In evaluating the success of the computer simulations one should note the following. There are, overall, three parameters: the concentration, the nearest-neighbor exchange and the intensity scaling factor. As discussed in Sec. II, for the 54% sample, chemical analysis on a separate sample from the same boule yields $c = 0.55 \pm 0.02$ while the percolation experiments discussed in Ref. 14 and Paper II suggest $c = 0.54 \pm 0.01$. Variation of c in the Alben-Thorpe theory by $\pm 2\%$ produces only a slight change in the theoretical spectra, although the optimal visual fit is indeed obtained for $c = 0.54$. Thus the concentration is not a bona-fide adjustable parameter although if one of the above estimates were grossly in error one might question some of the underlying assumptions. Choosing $c = 0.54$ for the first sample then necessitates $c = 0.57$ for the second; this value agrees exactly with the percolation experiment on the second sample. As is evident in Fig. 7, the computer simulations for $S^t(\vec{q}, \omega)$ ($c = 0.57$) at the zone boundary are also in very good agreement with the experiment.

The exchange interaction J_1 determines the horizontal scale factor for the theory. Using an nn-only spin-wave theory, one finds $J_1 = 0.65$ meV for Rb_2MnF_4 ($a = 4.214$ Å) and $J_1 = 0.75$ meV for K_2MnF_4 ($a = 4.16$ Å). Since $a \simeq 4.15$ Å for the random sample, one might have expected J_1 to be close to the K_2MnF_4 value. In fact, the optimal J_1 in the computer simulation is 0.72 meV, intermediate between the above two values. In the absence of an independent estimate of the true microscopic exchange, we can only comment that the value of J_1 deduced from the linear spin-wave theory is most reasonable. Finally, since we have not measured the scattering in absolute units one can only evaluate the success of the theory in predicting relative intensities. As noted above, with the intensity scale factor fixed by the zone boundary spectra, excellent agreement is obtained across the magnetic Brillouin zone. We note that much worse agreement[7] is found in the mixed magnetic system $Rb_2Mn_{0.5}Ni_{0.5}F_4$.

B. Coherent-potential approximation

The coherent-potential approximation is the analytic theory which is most frequently used to describe the excitations in disordered systems. There are two approaches which have been employed in its application to dilute antiferromagnets. The first approach by Buyers *et al.*[5] was based on the success of the Ising model in providing a qualitative understanding of the experimental results especially for wave vectors close to the zone boundary.[1] The Ising part of the magnetic interactions gives the characteristic excitation energy of each magnetic ion in its particular environment. The scattering of the excitations then arises because these energies are different for different environments and the effects of this scattering are calculated using the single-site CPA approximation[23] developed for electrons and phonons in alloys. The difficulty with this approach is in the treatment of the transverse parts of the magnetic interactions, and various different approximations[6] have been used to incorporate their effects at least approximately.

The second approach was developed by Harris *et al.*[24] to overcome the difficulty in treating the transverse interactions. They noticed that in dilute ferromagnets and antiferromagnets[25] the change in the Hamiltonian due to the presence of the nonmagnetic ions could be written as a sum over

the nonmagnetic sites. They were then able to include both the Ising and transverse parts of the exchange interactions in solving for the scattering of each nonmagnetic ion surrounded by its neighbors. Unfortunately, in this treatment all the magnetic ions are treated equivalently, and so there is no distinction made between magnetic ions surrounded by different numbers of nonmagnetic ions. As a result $S^t(\vec{Q}, \omega)$ has a single peak for each $\vec{Q}$, and the model fails to account for the fine structure shown in Figs. 4–7. Detailed calculations for the dilute (2-D) square lattice have not been made with this theory. Calculations have, however, been made[21] with the theory of Buyers *et al.*

Calculations were performed for a concentration $c = 0.5$ with nearest-neighbor-exchange interactions. Considerable difficulties were experienced with the convergence of the iterative procedure to obtain the coherent potential, and the results were obtained only after many (~40) iterations and using a reduction factor of 0.4 to reduce the calculated change in the coherent potential after each step. Even then, the potential had not completely converged for energies close to ±1.0 meV.

These calculations employed the same approximation to treat the transverse parts of the exchange interactions at Buyers *et al.*[5]; namely, that the frequency dependence of the off-diagonal part of the self-energy matrix was the same as that computed for the diagonal part. Because of the approximations inherent in the coherent potential approximation, it is necessary to ensure that the magnetic excitations do not propagate onto the nonmagnetic sites. One way of achieving this is to place a large repulsive potential at each nonmagnetic site[5,6] (hard core), and the other is to omit the nonmagnetic ions[6] (empty core). In Fig. 8, the results of both of these calculations, convoluted with the experimental resolution, are compared with the measured spectra. The calculations are only in qualitative accord with the measurements and give fine structure which is considerably more pronounced than that observed experimentally. This is clearly a much more severe test of the coherent potential approximation than earlier measurements for which the CPA theories appeared to be more successful as reviewed in Ref. 1. The reason for this may be the lower coordination number which makes the approximations inherent in the CPA more suspect, and which also makes measurements of the detailed spectral shape of $S^t(\vec{Q}, \omega)$ easier. We hope these measurements will lead to efforts to improve the CPA theories for these systems.

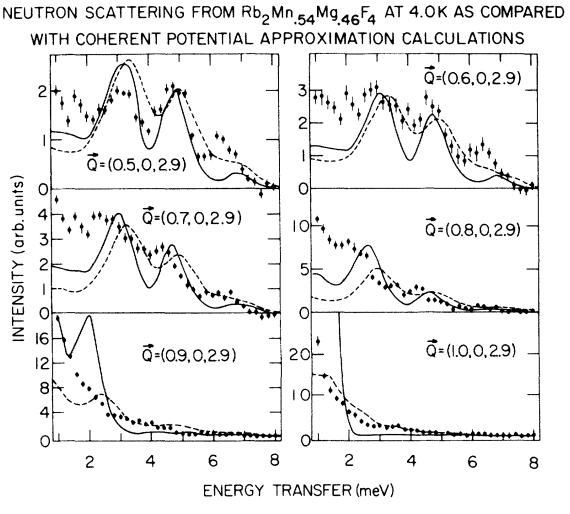

FIG. 8. Comparison of CPA theory for $S^t(\vec{Q}, w)$ with data for $Rb_2Mn_{0.54}Mg_{0.46}F_4$. The solid and dashed curves represent CPA calculations using the hard-core and empty-core approximations, respectively.

VI. CONCLUSIONS

In this paper we have presented measurements of the spin-wave excitations in pure Rb_2MnF_4 and the disordered materials $Rb_2Mn_cMg_{1-c}F_4$ with $c = 0.54 \pm 0.01$ and 0.57 ± 0.01. The results for the pure material show that the nearest-neighbor-exchange constant deduced from macroscopic measurements[20] is very accurately correct. There is also a weak antiferromagnetic next-nearest-neighbor-exchange constant.

In the disordered materials, the spin-wave excitations are damped to the extent that the scattering for each wave vector is spread over the whole of the spin-wave band. The weight, however, tends to lower frequencies near the zone center. The scattering does show considerably more marked structure than was observed[9] in the analogous 3-D materials. This structure arises from the different characteristic excitation energies of magnetic ions with different numbers of magnetic ions as neighbors. One of the most interesting aspects of our results is the excellent agreement obtained with computer simulations based on linear spin-wave theory.[3] This success shows that linear spin-wave theory does provide an appropriate description of the excitations in disordered as well as ordered magnetic materials. Analytic theories based on the coherent potential approximation are less successful at providing understanding of our results. Clearly our experiments suggest that further refinements of the CPA would be worthwhile. Finally, our

measurements show that the spin-wave spectra of the disordered materials is temperature dependent even below 10 K. We do not know of any theories of the temperature dependence of magnetic excitations in disordered systems.

ACKNOWLEDGMENTS

The computer program used to calculate the computer simulations was provided by Dr. R. Alben for whose assistance and encouragement we are grateful.

*Permanent address: Dept. of Physics, University of Edinburgh, Scotland.

†Work at Brookhaven performed under the auspices of the U.S. Energy Research and Development Agency.

‡Work at MIT supported by the NSF MRL Grant No. DMR12-03027-ADS.

[1]For a review, see R. A. Cowley, AIP Conf. Proc. 29, 243 (1976).

[2]W. Marshall and S. W. Lovesey, *Theory of Thermal Neutron Scattering* (Oxford U.P., New York, 1971).

[3]M. F. Thorpe and R. Alben, J. Phys. C 8, L275 (1975); 9, 2555 (1976).

[4]S. Kirkpatrick and A. B. Harris, Phys. Rev. B 12, 4980 (1975); W. K. Holcomb and A. B. Harris, AIP Conf. Proc. 24, 102 (1975); S. Kirkpatrick, *ibid.* 29, 141 (1976).

[5]W. J. L. Buyers, D. E. Pepper, and R. J. Elliott, J. Phys. C 5, 2611 (1972).

[6]G. J. Coombs and R. A. Cowley, J. Phys. C 8, 1889 (1975).

[7]J. Als-Nielsen, R. J. Birgeneau, H. J. Guggenheim, and G. Shirane, Phys. Rev. B 12, 4963 (1975); J. Phys. C 9, L121, (1976).

[8]G. J. Coombs, R. A. Cowley, W. J. L. Buyers, E. C. Svensson, T. M. Holden, and D. A. Jones, J. Phys. C 9, 2167 (1976).

[9]O. W. Dietrich, G. Meyer, R. A. Cowley, and G. Shirane, Phys. Rev. Lett. 35, 1735 (1975); E. C. Svensson, W. J. L. Buyers, T. M. Holden, and D. A. Jones, AIP Conf. Proc. 29, 248 (1976).

[10]For reviews, see V. K. S. Shante and S. Kirkpatrick, Adv. Phys. 20, 325 (1971); J. W. Essam, in *Phase Transitions and Critical Phenomena*, edited by C. Domb and M. S. Green (Academic, New York, 1972), Vol. II, p. 197.

[11]D. Stauffer, Z. Phys. 1322, 161 (1975); H. E. Stanley, R. J. Birgeneau, P. J. Reynolds, and J. F. Nicoll, J. Phys. C 9, L553 (1976); T. C. Lubensky, Phys. Rev. B 15, 311 (1977).

[12]D. J. Breed, K. Gilijamse, J. W. E. Sterkenberg, and A. R. Miedema, J. Appl. Phys. 41, 1267 (1970); Physica (Utr.) 68, 303 (1973).

[13]See, for example, S. Kirkpatrick, Phys. Rev. Lett. 36, 69 (1976), and references therein.

[14]R. J. Birgeneau, R. A. Cowley, G. Shirane, and H. J. Guggenheim, Phys. Rev. Lett. 37, 940 (1976); (unpublished).

[15]H. J. Guggenheim (unpublished).

[16]D. Balz and K. Pleith, Z. Elektrochem. 59, 545 (1955).

[17]R. J. Birgeneau, H. J. Guggenheim, and G. Shirane, Phys. Rev. B 1, 2211 (1970).

[18]H. W. de Wijn, L. R. Walker, and R. E. Walstedt, Phys. Rev. B 8, 285 (1973).

[19]D. E. Cox, G. Shirane, R. J. Birgeneau, and J. B. MacChesney, Phys. Rev. 188, 930 (1969).

[20]H. W. de Wijn, L. R. Walker, S. Geschwind, and H. J. Guggenheim, Phys. Rev. B 8, 299 (1973).

[21]H. Patterson, G. Shirane, and R. A. Cowley (unpublished).

[22]R. J. Birgeneau, H. J. Guggenheim, and G. Shirane, Phys. Rev. B 8, 304 (1973).

[23]P. Soven, Phys. Rev. 156, 809 (1967).

[24]A. B. Harris, P. L. Leath, B. G. Nickel, and R. J. Elliott, J. Phys. C 7, 1693 (1974).

[25]W. K. Holcomb, J. Phys. C 7, 4299 (1974).